Fast excited state dynamics in the isolated 7-azaindole-phenol H-bonded complex

Marcela C. Capello, Michel Broquier, Claude Dedonder-Lardeux, Christophe Jouvet, and Gustavo A. Pino

Citation: J. Chem. Phys. **138**, 054304 (2013); doi: 10.1063/1.4789426
View online: http://dx.doi.org/10.1063/1.4789426
View Table of Contents: http://jcp.aip.org/resource/1/JCPSA6/v138/i5
Published by the American Institute of Physics.

Fast excited state dynamics in the isolated 7-azaindole-phenol H-bonded complex

Marcela C. Capello,[1] Michel Broquier,[2,3] Claude Dedonder-Lardeux,[2,3,4] Christophe Jouvet,[2,3,4] and Gustavo A. Pino[1,a)]

[1]*Instituto de Investigaciones en Físico Química de Córdoba (INFIQC) CONICET – UNC. Dpto. de Fisicoquímica – Facultad de Ciencias Químicas – Centro Láser de Ciencias Moleculares - Universidad Nacional de Córdoba, Ciudad Universitaria, X5000HUA Córdoba, Argentina*
[2]*Centre Laser de l'Université Paris Sud (CLUPS, LUMAT FR 2764) Bât. 106, Univ Paris-Sud 11, 91405 Orsay Cedex, France*
[3]*Institut des Sciences Moléculaires d'Orsay (ISMO, UMR8624 CNRS) Bât. 210, Univ Paris-Sud 11, 91405 Orsay Cedex, France*
[4]*Physique des Interactions Ioniques et Moléculaires (PIIM): UMR-CNRS 7345 Aix-Marseille Université, Avenue Escadrille Normandie-Niémen, 13397 Marseille Cedex 20, France*

(Received 26 September 2012; accepted 11 January 2013; published online 5 February 2013)

The excited state dynamics of the H-bonded 7-azaindole-phenol complex (7AI-PhOH) has been studied by combination of picosecond pump and probe experiments, LIF measurements on the nanosecond time scale and *ab initio* calculations. A very short S_1 excited state lifetime (30 ps) has been measured for the complex upon excitation of the 0_0^0 transition and the lifetime remains unchanged when the ν_6 vibrational mode ($0_0^0 + 127\ cm^{-1}$) is excited. In addition, no UV-visible fluorescence was observed by exciting the complex with nanosecond pulses. Two possible deactivation channels have been investigated by *ab initio* calculations: first an excited state tautomerization assisted by a concerted double proton transfer (CDPT) and second an excited state concerted proton electron transfer (CPET) that leads to the formation of a radical pair (hydrogenated 7AIH$^\bullet$ radical and phenoxy PhO$^\bullet$ radical). Both channels, CDPT and CPET, seem to be opened according to the *ab initio* calculations. However, the analysis of the ensemble of experimental and theoretical evidence indicates that the excited state tautomerization assisted by CDPT is quite unlikely to be responsible for the fast S_1 state deactivation. In contrast, the CPET mechanism is suggested to be the non-radiative process deactivating the S_1 state of the complex. In this mechanism, the lengthening of the OH distance of the PhOH molecule induces an electron transfer from PhOH to 7AI that is followed by a proton transfer in the same kinetic step. This process leads to the formation of the radical pair (7AIH$^\bullet\cdots$PhO$^\bullet$) in the electronically excited state through a very low barrier or to the ion pair (7AIH$^+\cdots$PhO$^-$) in the ground state. Moreover, it should be noted that, according to the calculations the $\pi\sigma^*$ state, which is responsible for the H loss in the free PhOH molecule, does not seem to be involved at all in the quenching process of the 7AI-PhOH complex. © *2013 American Institute of Physics*. [http://dx.doi.org/10.1063/1.4789426]

I. INTRODUCTION

Reactions that involve coupled transfer of proton(s) and electron(s) (PCET) as well as the concerted proton-electron transfer in the same single kinetic step (CPET), are at the core of numerous chemical and biological systems.[1–5]

Many aspects of PCET and CPET, i.e.: kinetic isotope effect,[6,7] presence of inter- and intramolecular H-bonds,[8–11] proton donor-acceptor distance,[12] thermochemistry,[13] theoretical aspects,[14–16] etc., have been studied during the last years. The readers are referred to recent reviews on PCET and CPET that address all these topics.[1–4,14]

One of the most interesting examples in which PCET and CPET mechanisms are relevant is the oxidation of phenols (PhOHs) to phenoxy radicals (PhO$^\bullet$), because PhOH is the chromophore of the aminoacid tyrosine (TyOH) and tyrosyl radicals (TyrO$^\bullet$) which are extensively involved in Photosystem II,[17–20] prostaglandine H synthases 1 and 2,[21] cytochrome *c* oxidase,[22] galactose oxidase,[23] amine oxidases,[24] and other systems. Very recently, Bonin and Robert have reviewed the photo-induced PCET processes in biorelevant phenolic systems.[25]

In the gas phase it has been shown that excited state CPET plays a determinant role in the detailed mechanism of photostability of molecular building blocks of life. For instance, the ultrafast excited-state deactivation of biological molecules and supramolecular structures, such as DNA bases pairs, peptides, etc. has been suggested to be governed by a CPET along the intermolecular H-bonds.[26–28] Computational studies have shown that proton-transfer processes driven by charge-transfer (CT) states of $^1\pi\pi^*$, $^1n\pi^*$, or $^1\pi\sigma^*$ character, leading to a net hydrogen atom transfer (HAT) in the excited state (ESHAT), provide barrierless access to conical intersections between the locally excited-state and the ground-state

a)Author to whom correspondence should be addressed. Electronic mail: gpino@fcq.unc.edu.ar.

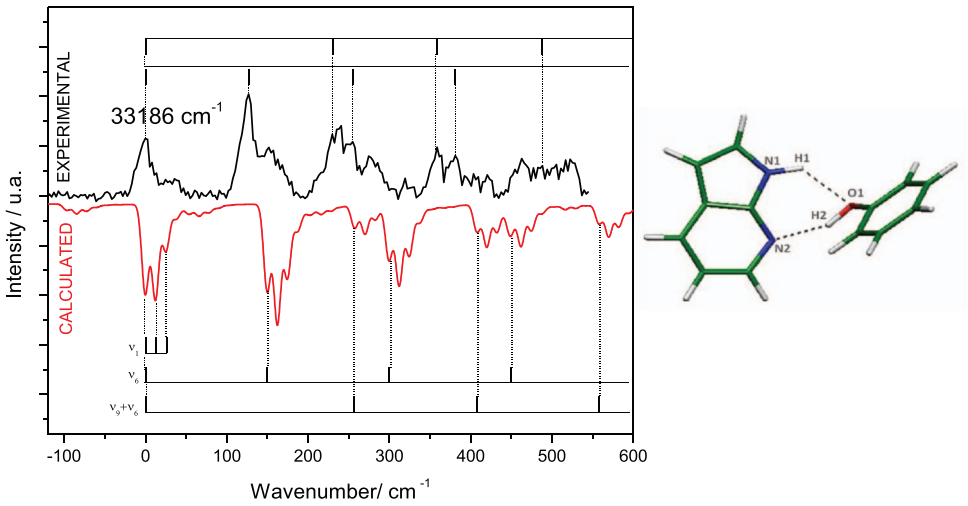

FIG. 1. (1 + 1) REMPI spectrum of 7AI-PhOH recorded with picosecond pulses (black trace). The lower spectrum (red trace) shows the Franck-Condon factors simulation of the electronic spectrum for this cluster with the vibrational frequencies calculated at the CC2 level, with the suggested assignment of some vibrational progressions.

potential energy surfaces (PESs), where ultrafast internal conversion (IC) takes place.[26,29–31]

A benchmark system to study ESHAT in the gas phase is the PhOH molecule and its H-bonded complexes with protic solvents such as NH_3 and H_2O.[29,32] In the case of $PhOH(NH_3)_n$ complexes the potential energy function of the locally excited $\pi\pi^*$ state is crossed by the $\pi\sigma^*$ function whose energy is strongly stabilized when the proton moves from PhOH to NH_3. At the ground state equilibrium geometry the σ^* orbital is already located on the ammonia molecule to a substantial extent, indicating that the $\pi\sigma^*$ state has a CT character. At the equilibrium geometry of the $\pi\sigma^*$ state, the proton has followed the electron, resulting in the formation of a radical pair.[29–31] In addition, for a number of substituted PhOHs it has been shown that the energy gap between the $\pi\sigma^*$ and $\pi\pi^*$ states determines the rate of the ESHAT reaction which takes place through tunnel effect.[33]

Although the ESHAT mechanism can explain the photochemistry of several aromatic molecules of biological relevance with OH or NH groups, an interesting case is presented by 7-azaindole (7AI), a model molecule for DNA bases. This molecule has a H-acceptor nitrogen atom in the six member ring and a H-donor nitrogen atom in the five member ring. Upon electronic excitation, the basicity of the nitrogen atom in the six member ring increases together with the acidity of the nitrogen atom in the five member ring. In the gas phase, it has been shown that when both nitrogen atoms are connected by a H-bonded molecular wire of two H_2O,[34,35] CH_3OH,[36,37] CH_3CH_2OH[38] molecules or in the case of the H-bonded $(7AI)_2$ dimer[39] and other substituted 7AI dimers,[40] the increased basicity and acidity of the two sites trigger the excited state tautomerization of 7AI. Vibrational mode selective tautomerization dynamics was experimentally observed from frequency-resolved,[34,37,38] and picosecond pump and probe experiments.[35] Excited state *ab initio* calculations suggest that the vibrational mode selective tautomerization mechanism in all the above mentioned complexes is due to a concerted double or triple proton transfer, while the electron remains in the π^* orbital of the chromophore. Thus, the 7AI molecule becomes a special case in which the ESHAT is unlikely to take place in the excited state when both functional groups are connected by intermolecular H-bonds.

While the excited state dynamics of PhOH has become a prototype for ESHAT, the excited state tautomerization of 7AI assisted by intermolecular H-bonds seems to be a prototype for excited state concerted multiple proton transfer. Therefore, the excited state dynamics and spectroscopy of the 7AI-PhOH complex seems to be a good example to study the competition between these processes.

In this regard, the 7AI-PhOH complex, in which the PhOH molecule acts as a molecular bridge between the pyrrolic NH group and the pyridinic N group (Figure 1), has been recently investigated in methylcyclohexane solutions by stationary UV-visible absorption and fluorescence spectroscopy.[41] The complexation of 7AI with PhOH resulted in a dramatic quenching of the 7AI fluorescence in the UV spectral region due to the opening of a non-radiative deactivation channel, without the appearance of visible emission from the tautomer. This result is evidence for the quenching of the H-bonded assisted excited state tautomerization by PhOH, although this process is accelerated by C_2H_5OH and CH_3OH. The authors suggested that excited state PCET is likely to be responsible for the fluorescence and tautomerization quenching.

In this work, we present a study on the excited state dynamics of the 7AI-PhOH complex in the gas phase by combination of nanosecond REMPI and LIF spectroscopy with time resolved pump and probe picosecond spectroscopy and quantum chemistry calculations. The possible reactive mechanisms are explored by high level *ab initio* calculations and their accuracy is monitored by comparison between calculation and spectroscopic information.

II. EXPERIMENTAL

The experimental setup used in Orsay for the experiments with picosecond laser pulses has been described previously.[33] Briefly, 7AI-PhOH clusters were generated by co-expanding

a mixture of He, 7AI, and PhOH. Products were purchased from Sigma-Aldrich and used without further purification. The carrier gas He at a backing pressure of 1.5 bars passed through two reservoirs, the first one containing PhOH at room temperature and the second one containing 7AI heated at 358 K. The gas mixture was expanded into a vacuum chamber through a 300 μm diameter pulsed nozzle (Solenoid General Valve, Series 9). Under these conditions, structured vibronic REMPI (1 + 1) spectra were obtained.

The skimmed free jet was crossed at right angles by the laser beams, 10 cm downstream from the nozzle. The interaction region was the center of the extraction zone of a linear time-of-flight (TOF) mass spectrometer. The produced ions were accelerated perpendicularly to the jet axis toward a microchannel plates detector located at the end of a 1.5 m field-free flight tube.

For the pump-probe experiments, the third harmonic (355 nm) output of a mode-locked picosecond Nd:YAG laser (EKSPLA-SL300) was split in two parts to pump two OPA and SHG systems (EKSPLA-PG411) to obtain tunable UV light. One of the systems was used as the excitation laser (ν_1) and scanned while the other system was tuned to 306 nm and used as the ionization laser (ν_2), keeping its energy to approximately 100 μJ/pulse while the energy of the ν_1 laser was attenuated to preclude one-color two-photon ionization. The temporal shapes of both pulses were determined in the fitting procedure as Gaussian functions of (15 ± 2) ps FWHM,[33] while the spectral line width was 5 cm^{-1}. The laser pulses were optically delayed between −200 ps and 500 ps by a motorized stage.

The setup used in Córdoba for LIF and REMPI spectroscopy with nanosecond lasers were essentially the same as described previously,[42] and the experimental conditions were the same as for the experiments performed in Orsay. The LIF and REMPI spectra were measured using a frequency doubled Lumonics (HD5000) dye laser (FWHM = 5 ns) operating with a mixture of Rhodamine 590 and 610, pumped by the second harmonic of a Spectra-Physics (Indi-HG) Nd:YAG laser. For the LIF experiments, the fluorescence from the clusters was detected by a photomultiplier tube (PMT) (Hamamatsu R636) without any filters. In the case of the REMPI experiments, the ions were extracted with a home-built Wiley-McLaren type TOF mass spectrometer (46 cm of length), perpendicular to the molecular beam and laser directions, and entered the drift chamber, where they were detected with microchannel plates. The signals from the PMT and the MCP were averaged and digitized by a Tektronic (TDS-3034B) oscilloscope and integrated with a PC. The rise time of the complete detection system was 1 ns.

III. THEORETICAL CALCULATIONS

Ab initio calculations were performed with the TURBOMOLE® program package,[43] making use of the resolution-of-the-identity (RI) approximation for the evaluation of the electron-repulsion integrals.[44] The equilibrium geometry of the clusters in their ground electronic state (S_0) was determined at both the MP2 level. Excitation energy and equilibrium geometry of the lowest excited singlet state (S_1) were determined at the RI-CC2 level.[45] Calculations were performed with the correlation-consistent polarized valence double-zeta basis set (cc-pVDZ).[46] The Franck-Condon simulations were performed using the PGOPHER software.[47]

IV. RESULTS AND DISCUSSION

A. Picosecond experiments

The REMPI (1 + 1) spectrum of the 7AI-PhOH complex (Figure 1) was recorded with picosecond laser pulses in the spectral region (33 000-33 750) cm^{-1} by integrating the signal recorded on the ion mass (212 amu).

The band origin (0_0^0) for the $S_1 \leftarrow S_0$ electronic transition of the complex appears at 33 186 cm^{-1} (4.12 eV) and well-defined progressions of low-energy vibronic modes are observed. The electronic absorption is shifted by 1448 cm^{-1} to lower energy as compared to the free 7AI transition.[48]

The excited-state lifetimes of the 7AI-PhOH complex were determined upon excitation of the 0_0^0 (33 186 cm^{-1}) and $0_0^0 + 127$ cm^{-1} (33 313 cm^{-1}) bands. Typical time dependent pump and probe signals recorded upon excitation of these two transitions (on-resonance signals) are shown in Figure 2. In addition, the corresponding off-resonance signals that account for the dynamics of larger clusters recorded with the pump laser set slightly to the red of the bands (at 33 000 cm^{-1} and 33 220 cm^{-1}, respectively) are also depicted in Figure 2. Finally, the results of the subtraction of the off-resonance signals from the on-resonance signals, which account for the dynamics of the 7AI-PhOH complex are shown in Figure 2 with their corresponding fittings to a function which is the convolution of the temporal profile of the lasers pulses with an exponential decay function. The excited state lifetimes determined for both vibronic states were (30 ± 10) ps. These values are not very precise because they are close to the temporal resolution of the experimental setup (15 ± 2) ps. However, it is clear that the excited state lifetime does not depend *strongly* on the vibrational mode excited as observed in other similar systems[33–35,37] in which the reaction rate becomes at least twice or three times faster when an intermolecular vibrational mode along the reaction coordinate is excited. These results indicate a lack of vibrational specificity of the vibrational mode ν_6 (vide infra) at $0_0^0 + 127$ cm^{-1} (33 313 cm^{-1}) in the present system and then, that this mode is not connected to the reaction coordinate.

B. Fluorescence excitation spectra with nanosecond laser

The short excited state lifetimes, determined by pump and probe ionization, could be due to a tautomerization or isomerization process that produces an electronically excited specie with a higher ionization potential as in the case of the $7AI(H_2O)_3$ complex[35] where the final complex cannot be ionized with the same ionization photon as the initial complex but may still fluoresce. The other possibility is that the excited state lifetime is linked to a non-radiative process that populates a dark state.

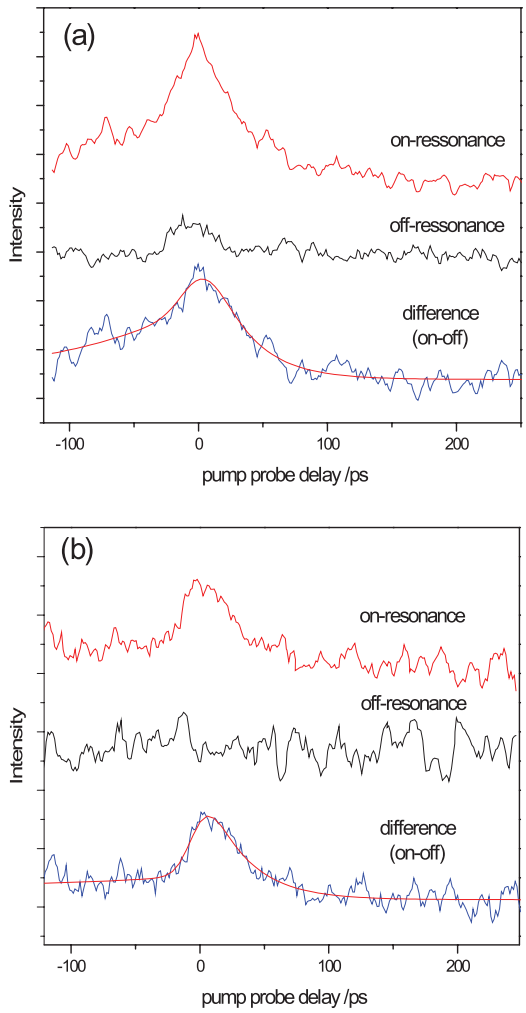

FIG. 2. Pump and probe signals recorded on the mass channel of the 7AI-PhOH$^+$ ion, upon excitation to the 0_0^0 transition (a) and to the 0_0^0 +127 cm^{-1} transition (b). The probe wavelength was 306 nm. Upper trace: on-resonance excitation; middle trace: off-resonance excitation; and bottom trace: difference between on-resonance and off-resonance signals with their respective fitting to a pulse shape convoluted single exponential decay function.

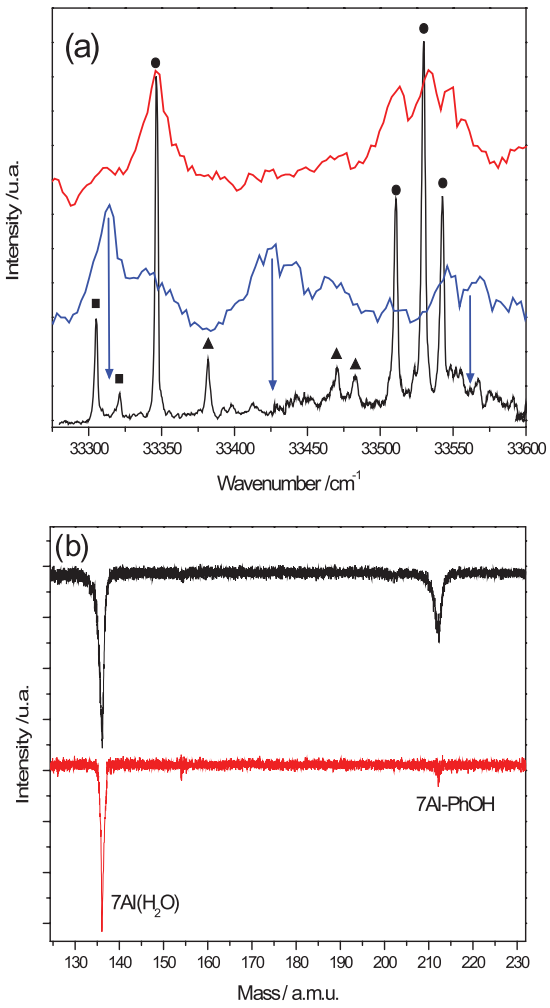

FIG. 3. (a) LIF spectrum measured by exciting with nanosecond pulses and detecting the total UV-vis fluorescence (black). The circles, triangles, and squares indicate the vibronic bands of the 7AI(H$_2$O), 7AI(H$_2$O)$_2$, and 7AI(H$_2$O)$_3$ complexes, respectively. REMPI spectra of 7AI-PhOH (blue) and 7AI(H$_2$O)$_1$ (red) recorded with picosecond pulses, for comparison. (b) Mass spectrum recorded under the same experimental conditions that the LIF spectrum. The ionization was achieved with nanosecond pulses with the laser tuned on-resonance at 33 313 cm^{-1} (upper trace) and off-resonance at 33 250 cm^{-1} (lower trace).

Therefore, further information on the excited state dynamics of the 7AI-PhOH complex can be obtained from fluorescence experiments. The LIF spectrum in the (33 275-33 600) cm^{-1} spectral range (Figure 3(a)), was collected under the same expansion conditions as in the picosecond experiments by recording the total UV-visible fluorescence. The transitions observed were assigned by comparison with previous reports[34,35,48] to the 7AI(H$_2$O)$_n$ (n = 1, 2, and 3) complexes, produced as a consequence of the humidity in the experimental setup. The same transitions were observed in the REMPI spectra recorded with the picosecond lasers by integrating the ion mass peaks at 136 amu, 154 amu, and 172 amu corresponding to the 1:1, 1:2, and 1:3 water complexes, respectively. The expected positions of 7AI-PhOH bands are marked with arrows and compared with the REMPI spectrum recorded with the picosecond lasers, but the transitions are not detectable on the background signal of the LIF spectrum.

The TOF mass spectra (Figure 3(b)) were recorded simultaneously with the LIF spectrum with the excitation laser tuned on-resonance with the 0_0^0 + 127 cm^{-1} (33 313 cm^{-1}) transition (upper trace) and off-resonance at 33 250 cm^{-1} (lower trace). Although the signal of the 7AI-PhOH complex in the mass spectrum is low, it can be resonantly excited. The larger signal for the non-resonant excitation of the 7AI(H$_2$O) complex is due to larger excited state lifetime (8.1 ns)[48] of this complex as compared to that of the 7AI-PhOH complex (30 ps).

These spectra give evidence that although the complex is produced in the molecular beam and is excited and ionized with nanosecond lasers, the fluorescence quantum yield, if any, is very low and the excited state dynamics is governed by a non-radiative decay process that yields a non-fluorescent product.

The effect of deuteration on the fluorescence yield was also checked by flowing He seeded with D_2O. After 30 min the mass spectrum showed the appearance of masses 213 amu and 214 amu corresponding to the 7AI-PhOH(d_1

and d_2) complexes. Although many efforts were devoted to record the LIF spectrum for the deuterated complexes we were unable to detect any fluorescence signal on the background.

C. The vibronic analysis

The first electronic transition calculated starts from the $\pi\pi$ S_0 state to a $\pi\pi^*$ S_1 state. Figure 1 shows the vibronic spectrum simulated (red trace) through *ab initio* frequency calculations and Franck-Condon analysis and the comparison with the experimental spectrum.

The band origin calculated from excited state optimization with correction for the difference in zero point energies between the ground and the excited states δZPE at the RI-MP2/CC2-basis set cc-pVDZ level is 4.03 eV, which is quite close to the experimental value of 4.11 eV. Such a reasonable agreement is quite common with this method[33,35,49,50] and gives good confidence on the calculations for the potential energy surface done to understand the dynamical processes. The calculated vibrational spectrum is also in good agreement with the experimental one, although the calculated frequencies seem to be overestimated.

The calculated vibronic spectrum is built on three active vibrational modes which are depicted in Figure 4. The lowest energy mode of 15 cm^{-1} in S_0 and 13 cm^{-1} in S_1, which corresponds to a butterfly movement as shown in Figure 4(a), cannot be resolved experimentally due to the spectral width of the laser. The second mode ν_6 with a frequency of 150 cm^{-1} in S_1 is linked to the stretching of the N1H1···O1 hydrogen bond distance (Figure 4(b)). The activity of this mode is reflecting the shortening of the H1···O1 distance from 2.09 Å to 1.85 Å upon electronic excitation as in other PhOH[33,51] and 7AI[34–38] complexes. The optimized geometries and relevant bond distances of the complex in the S_0 and S_1 states are available in the supplementary material.[52]

The third mode ν_9 with a frequency of 258 cm^{-1} in S_1 is also linked to the N1H1···O1 stretching mode (Figure 4(c)). From these calculated frequencies the experimental spectrum can be partly assigned as shown in Figure 1 and Table I. It should be noticed that none of these modes is connected to the O1H2···N2 coordinate involved in the CPET mechanism (vide infra).

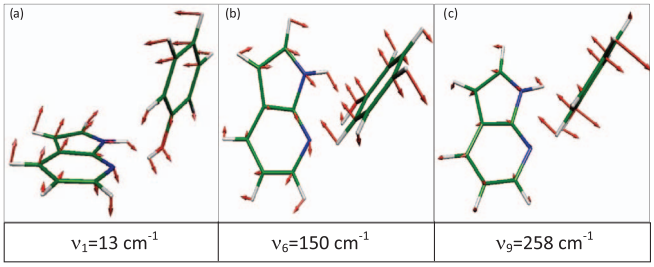

FIG. 4. Low frequency (a) 13 cm^{-1}, (b) 150 cm^{-1}, and (c) 258 cm^{-1} vibrational normal modes of the 7AI-PhOH complex, calculated at the RI-CC2/basis set pVDZ level.

TABLE I. Experimental and calculated vibrational frequencies of the S_1 state of 7AI-PhOH.

Vibrational assignment	Calculated vibrational energy/cm^{-1}	Experimental spectrum assignment/cm^{-1}
Origin	0 (32 540 cm^{-1})	0 (33 186 cm^{-1})
$1\nu_1$	13	...
$2\nu_1$	26	...
$1\nu_6$	150	127
$1\nu_9$	257	230
$2\nu_6$	300	255
$1\nu_9 + 1\nu_6$	407	358
$3\nu_6$	450	381
$1\nu_9 + 2\nu_6$	557	488

D. The non-radiative pathways

The short lifetime measured in the experiment is an evidence of a fast dynamics occurring in the excited state. On the basis of previous studies on 7AI H-bonded complexes,[34–40] we have investigated two possible channels:

(1) A concerted double proton transfer (CDPT) in which the N1H1 from 7AI as well as the O1H2 from PhOH are stretched together in order to lead to the excited state tautomerization as in the case of $7AI(H_2O)_2$,[34,35] $7AI(CH_3OH)_2$,[36,37] or $7AI(C_2H_5OH)_2$.[38] In this reaction path, the reaction coordinate is the synchronous lengthening of the N1H1 and O1H2 bond distances and is associated with the ν_6 and ν_9 vibrational modes.

(2) A single proton or HAT from the O1H2 group of PhOH to the pyridine N2 of 7AI. This process leads to the formation of either an ion pair or a radical pair structure and the reaction coordinate is mainly the O1H2 bond distance.

1. Concerted double proton transfer

The minimum energy path corresponding to the CDPT is presented in Figure 5. Here the two N1H1 and O1H2 distances are stretched simultaneously and at each step the other coordinates are optimized. The minimum energy path does not show any sign of states crossing, and the orbitals involved in the $S_1 \leftarrow S_0$ electronic transition stay the same all along the path ($\pi\pi^*$ state).

The potential energy curve is very similar to the one calculated for $7AI(H_2O)_2$.[34] A barrier of 0.14 eV is evidenced in the present case, which is lower than in the case of $7AI(H_2O)_2$ (0.2 eV)[34] and $7AI(CH_3OH)_2$ (0.2 eV).[34] As pointed out by Fang *et al.*,[53] this path is not necessary the lowest in energy and can be even lower if the N1H1 and O1H2 distance are not equally stretched. In the S_0 state and in the optimized S_1 state geometries, only the O1H2 bond is in the 7AI plane, the rest of the PhOH molecule being out of the plane of the 7AI molecule. As a consequence, the phenyl ring rotates simultaneously with the CDPT in order to obtain the O1H1 group in the plane of the phenyl ring at the end of the tautomerization. This pathway involves the displacement of the relatively

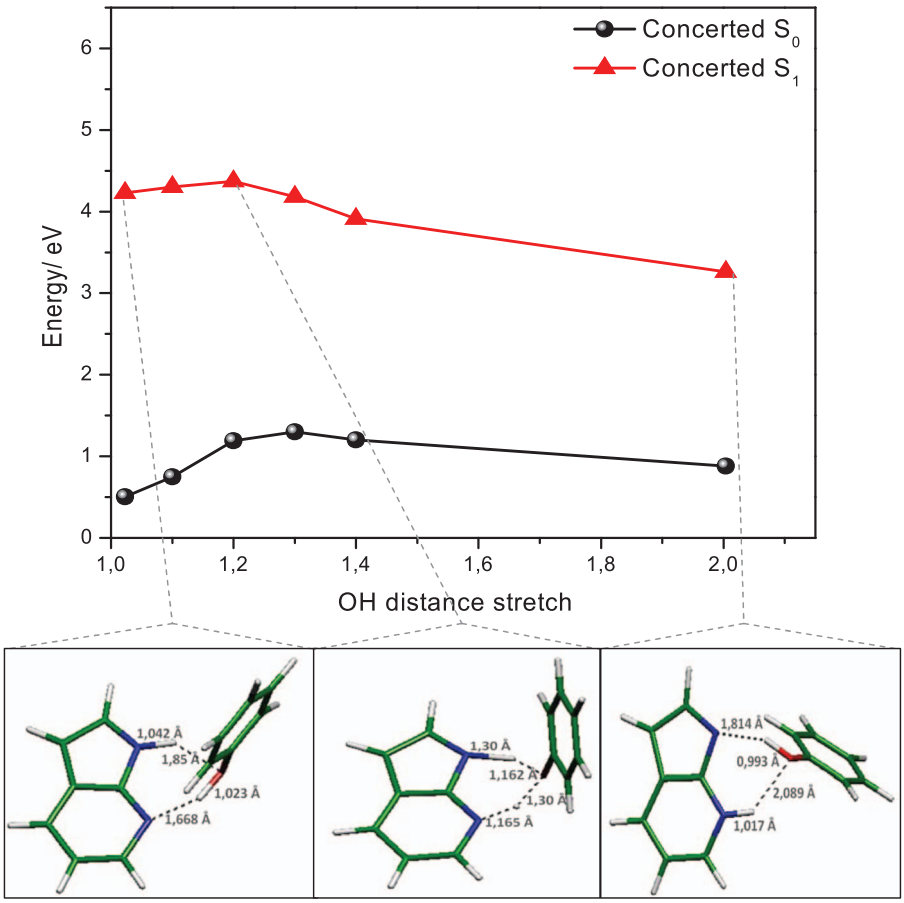

FIG. 5. Potential energy functions for the electronic ground state (S_0) and the locally excited (S_1) state of the 7AI-PhOH as a function of the concerted stretching of the O1H2/N1H1 distances. The optimized structures in different regions of the excited states function are shown in the lower part of the figure.

heavy phenyl ring and thus cannot be achieved only by tunneling of the light protons.

2. Single proton or hydrogen atom transfer

The second pathway that we have investigated is the HAT from the O1H2 group of PhOH to the pyridine N2 of 7AI. In this approach only the O1H2 coordinate is involved in the minimum energy scan of the potential energy surfaces. The potential energy functions along the reaction coordinate were built by stretching the O1H2 bond by steps of 0.1 Å or 0.05 Å and optimizing the other degrees of freedom, starting from the S_1 optimized structure. The potential energy functions calculated as described above for the S_0, $\pi\pi^*$, and CT states are shown in Figure 6.

The potential energy of the $\pi\pi^*$ state (the first excited state at the vertical excitation geometry) increases as the O1H2 coordinate is elongated. At the opposite the energy of the CT state in which an electron from the π orbital of PhOH is promoted to the π^* orbital of 7AI lowest unoccupied molecular orbital (LUMO) strongly decreases. This CT state is the fifth electronic state at the S_1 equilibrium geometry with an energy value of 6.33 eV. At a distance between 1.20 Å and 1.25 Å, the energy curve of the CT state crosses the energy curve of the $\pi\pi^*$ state and the CT state becomes the lowest excited state. This crossing corresponds to a change in the highest occupied molecular orbital (HOMO): in the $\pi\pi^*$ state the HOMO as well as the LUMO are localized on the π and π^* orbitals of 7AI molecule, respectively, whereas in the CT state the HOMO is localized on the π orbital of PhOH while the LUMO is the same π^* orbital of 7AI as in the $\pi\pi^*$ state.

When the O1H2 distance is further elongated, the energy of the CT state continues decreasing, and if the system is optimized in releasing the constraint, the proton follows the electron and attaches to the N2 atom leading to the radical pair $7AIH^{\bullet}\cdots PhO^{\bullet}$, which is equivalent to a HAT from PhOH to 7AI. This optimization leads to a T shaped structure lower in energy than the initial optimized $\pi\pi^*$ structure[52] by 1.6 eV. In the ground state of this structure, the highest doubly occupied orbital is localized on the PhO moiety, which corresponds to the phenoxy anion (PhO^-), while in the excited state one electron is promoted from this HOMO on PhO^- towards the LUMO, a π^* orbital on the protonated $7AIH^+$ moiety (see Figure 6, lower part). In this final structure, the ground and excited state are very close in energy ($\Delta E = 0.14$ eV), thus a conical intersection between the ground and excited state is highly probable, and this would induce a fast non-radiative decay.

On this pathway, a transition state has been found with an O1H2 distance of 1.160 Å while the N1H1 distance is 1.04 Å.[52] The electronic nature of the excited state at this

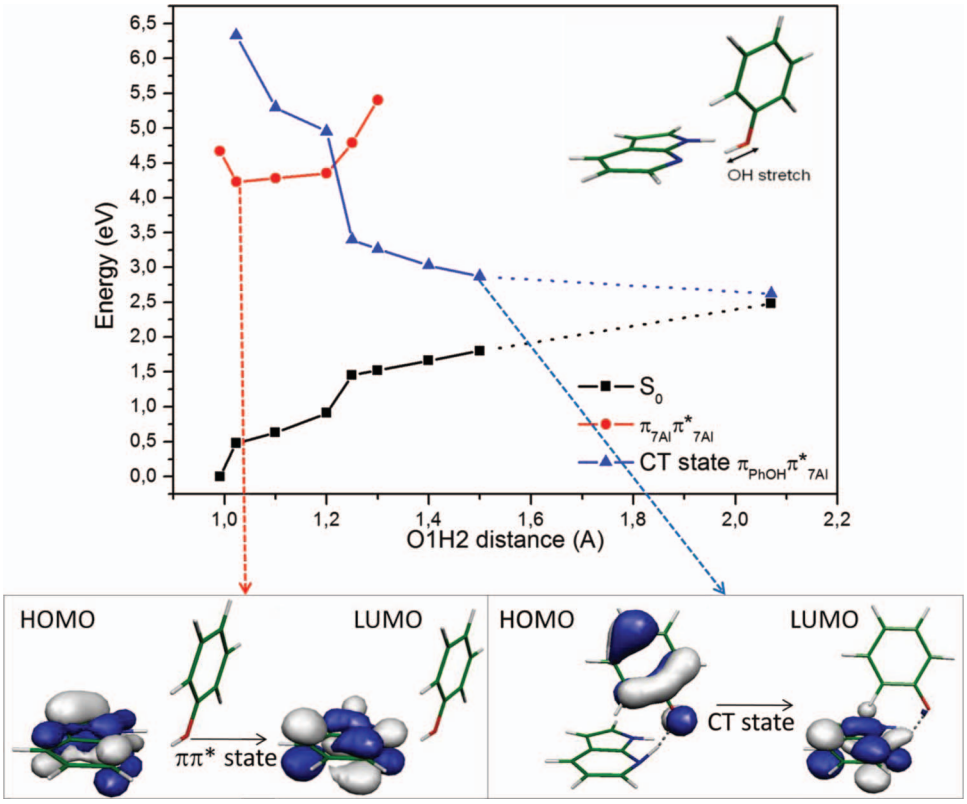

FIG. 6. Potential energy function for the electronic ground state (S_0), the locally excited ($\pi\pi^*$), and the charge-transfer excited (CT) states of the 7AI-PhOH, as a function of the O1H2 distance. The scheme of the orbitals involved in the transitions for the $\pi\pi^*$ and CT states are shown in the lower part of the figure.

geometry has still mainly a $\pi\pi^*$ character on 7AI but it is mixed with a CT configuration (π(PhOH)-π^*(7AI)). The height of the barrier is 0.12 eV (without δZPE correction), which is quite small and can be probably overcome through tunneling effect, leading to a fast excited state deactivation and then a short excited state lifetime.

We have also investigated the minimum energy pathway when the N1H1 bond is stretched and the other coordinates are optimized. As soon as the N1H1 distance is 1.2 Å the optimization process leads to the attachment of the H2 atom to the N2 atom and to the formation of the same radical pair obtained by stretching the O1H2 bond.

It should be noted that this HAT or CPET process is dynamically different from the standard ESHAT observed in PhOH$(NH_3)_n$ complexes[29,31,33] in the sense that it does not involve the $\pi\sigma^*$ state which is also responsible for the H loss in the free PhOH molecule.[29,54] The $\pi\sigma^*$ state may play a role at higher excitation energies and it might be worthwhile to investigate this point in the future.

The analysis of the whole experimental and theoretical data allows us to conclude that the excited state tautomerization assisted by CDPT is unlikely to be responsible for the very short excited state lifetime on the basis of the following evidence:

(1) The lack of variation of the excited lifetime upon excitation of the vibrational mode ν_6 associated with the CDPT reaction coordinate as expected by comparison with related systems (i.e., the excitation of the intermolecular stretching (σ mode) in PhOH-NH_3 complex[33,51] or the modes at 228 cm^{-1} in the 7AI-$(CH_3OH)_2$ complex[37] or at 175 cm^{-1} in the 7AI-$(H_2O)_2$ complex.[34,35]

(2) The absence of or negligible UV-visible fluorescence from the tautomer, as compared with related 7AI$(H_2O)_2$ complex, that we measured simultaneously and for which tautomerization assisted by CDPT has been demonstrated previously.

(3) In addition, calculations indicate that this mechanism requires the rotation of the relatively heavy phenyl ring simultaneously with the CDPT which cannot be achieved by tunneling of the energy barrier.

On the other hand the HAT or CPET, in which the stretching of the O1H2 distance induces an electron transfer from the π orbital of PhOH to the π^* orbital of 7AI accompanied by a proton transfer from PhOH to 7AI, can be accessed through a low barrier that can be tunneled by the proton in agreement with the fast decay observed. The diradical formation may be followed by a second crossing to a ground state ion pair, which can explain the absence of fluorescence in both jet and condensed phase.[41] Finally, the ν_6 mode associated to the N1H1···O1 intermolecular stretching is not connected to the O1H2···N2 reaction coordinate of the CPET. Thus, one does not expect any variation on the reaction rate (or excited state lifetime) when this intermolecular mode is excited, in good agreement with the lack of vibrational specificity upon excitation of this mode.

It should be mentioned that the calculations performed in this paper represent only the exploration of a small fraction of

the full PES and it might be that other non-radiative pathways have lower barrier. One also has to consider that, although CC2 gives good results near the equilibrium geometry, this is not the best method to treat properly conical intersections[55] which seem to be present in the processes. We hope that this preliminary approach will trigger more theoretical work using other *ab initio* methods, scanning a larger part of the PES and performing dynamics studies such as wave packet propagation.

V. CONCLUSIONS

The excited state dynamics of aromatic molecules containing hetero atoms is quite rich, especially when linked to H-bonded systems with OH or NH bond, varying from simple H loss mediated by Rydberg $\pi\sigma^*$ states in the free molecules[54] as well as in the clusters,[29,31,33] to the sequential excited state proton transfer like in $7HQ(NH_3)_3$[56] or else to concerted double proton transfer as in the $7AI(H_2O)_2$,[34,35] $7AI(CH_3OH)_2$,[36,37] or $7AI(C_2H_5OH)_2$[38] complexes.

In the present 7AI-PhOH system, two competing channels, the concerted proton electron transfer leading to hydrogen atom transfer and the concerted double proton transfer leading to the tautomerization seem to be energetically open according to *ab initio* calculations. However, the absence of fluorescence and the lack of vibrational specificity of the excited state lifetime upon excitation of the reaction coordinate allow us to exclude a tautomerization reaction and thus the concerted double proton transfer mechanism seems unlikely, which leaves the concerted proton electron transfer reaction as the probable mechanism involved in the fast decay observed for the excited electronic state.

We hope that the data and the calculations reported here will trigger more theoretical work on this system which can then be used as a benchmark to test the different theoretical approach used to model the CPET mechanism.[6,14–16]

ACKNOWLEDGMENTS

The authors thank Professor M. Fujii for helpful discussion. This work was supported by MinCyT-Córdoba, ANPCyT-FONCYT (PICT2010 – 708), CONICET (PIP11220090100436), SeCyT-UNC, Université Paris–Sud 11, by the ANR research grant (Grant No. NT05-1 44224), and the CNRS/CONICET and MinCyT-ECOS (Grant No. A11E02) exchange programs. The calculations have been performed on the GMPCS cluster of LUMAT.

[1] J. M. Mayer, Annu. Rev. Phys. Chem. **55**, 363 (2004), and references therein.
[2] M. H. V. Huynh and T. J. Meyer, Chem. Rev. **107**, 5004 (2007), and references therein.
[3] D. Weinberg, C. Gagliardi, J. Hull, C. F. Murphy, C. A. Kent, B. C. Westlake, A. Paul, D. Ess, D. G. McCafferty, and T. J. Meyer, Chem. Rev. **112**, 4016 (2012), and references therein.
[4] J. M. Mayer, Acc. Chem. Res. **44**, 36 (2011).
[5] S. Hammer-Schiffer, Chem. Rev. **110**, 6937 (2010).
[6] A. Hazra, A. Soudackov, and S. Hammes-Schiffer, J. Phys. Chem. Lett. **2**, 36 (2011).
[7] J. Bonin, C. Costentin, C. Louault, M. Robert, M. Routier, and J. M. Savéant, Proc. Natl. Acad. Sci. U.S.A. **107**, 3367 (2010).
[8] I. J. Rhile, T. F. Markle, H. Nagao, A. G. DiPaqueale, O. P. Lam, M. A. Lockwood, K. Rotter, and J. M. Mayer, J. Am. Chem. Soc. **128**, 6075 (2006).
[9] J. Bonin, C. Costentin, M. Robert, J. M. Savéant, and C. Tard, Acc. Chem. Res. **45**, 372 (2012).
[10] A. Pizano, J. L. Yang, and D. Nocera, Chem. Sci. **3**, 2457 (2012).
[11] T. Alligrant and J. Alvarez, J. Phys. Chem. C **115**, 10797 (2011).
[12] T. F. Markle, I. J. Rhile, and J. M. Mayer, J. Am. Chem. Soc. **133**, 17341 (2011).
[13] J. J. Warren, T. A. Tronic, and J. M. Mayer, Chem. Rev. **110**, 6961 (2010).
[14] S. Hammes-Schiffer and A. A. Stuchebrukhov, Chem. Rev. **110**, 6939 (2010), and references therein.
[15] S. Hammes-Schiffer, E. Hatcher, H. Ishikita, J. H. Skone, and A. V. Soudackov, Coord. Chem. Rev. **252**, 384 (2008).
[16] J. H. Skone, A. V. Soudackov, and S. Hammes-Schiffer, J. Am. Chem. Soc. **128**, 16655 (2006).
[17] S. Y. Reece and D. G. Nocera, Annu. Rev. Biochem. **78**, 673 (2009).
[18] C. J. Gagliardi, B. C. Westlake, C. A. Kent, J. J. Paul, J. M. Papanikolas, and T. J. Meyer, Coord. Chem. Rev. **254**, 2459 (2010).
[19] B. A. Barry and G. T. Babcock, Proc. Natl. Acad. Sci. U.S.A. **84**, 7099 (1987).
[20] T. J. Meyer, M. H. V. Huynh, and H. H. Thorp, Angew. Chem., Int. Ed. **46**, 5284 (2007).
[21] A. L. Tsai, G. Palmer, G. Xiao, D. C. Swinney, and R. J. Kulmacz, J. Biol. Chem. **273**, 3888 (1998).
[22] V. R. I. Kaila, M. I. Verkhovsky, and M. Wikström, Chem. Rev. **110**, 7062 (2010).
[23] M. M. Whittaker and J. W. Whittaker, J. Biol. Chem. **265**, 9610 (1990).
[24] S. M. Janes, D. Mu, D. Wemmer, A. J. Smith, S. Kaur, D. Maltby, A. L. Burlingame, and J. P. Klinman, Science **248**, 981 (1990).
[25] J. Bonin and M. Robert, Photochem. Photobiol. **87**, 1190 (2011), and references there in.
[26] Z. Lan, L. M. Frutos, A. Sobolewski, and W. Domcke, Proc. Natl. Acad. Sci. U.S.A. **105**, 12707 (2008).
[27] E. Samoylova, V. R. Smith, H.-H. Ritze, W. Radloff, M. Kabelac, and T. Schultz, J. Am. Chem. Soc. **128**, 15652 (2006).
[28] A. Abo-Riziq, L. Grace, E. Nir, M. Kabelac, P. Hobza, and M. S. de Vries, Proc. Natl. Acad. Sci. U.S.A. **102**, 20 (2005).
[29] A. L. Sobolewski, W. Domcke, C. Dedonder-Lardeux, and C. Jouvet, Phys. Chem. Chem. Phys. **4**, 1093 (2002).
[30] A. L. Sobolewski and W. Domcke, J. Phys. Chem. A **111**, 11725 (2007).
[31] W. Domcke and A. L. Sobolewski, Science **302**, 1693 (2003).
[32] G. Pino, G. Grégoire, C. Dedonder-Lardeux, C. Jouvet, S. Martrenchard, and D. Solgadi, Phys. Chem. Chem. Phys. **2**, 893 (2000).
[33] G. A. Pino, A. N. Oldani, E. Marceca, M. Fujii, S.-I. Ishiuchi, M. Miyazaki, M. Broquier, C. Dedonder, and C. Jouvet, J. Chem. Phys. **133**, 124313 (2010).
[34] K. Sakota, C. Jouvet, C. Dedonder, M. Fujii, and H. Sekiya, J. Phys. Chem. A **114**, 11161 (2010).
[35] G. A. Pino, I. Alata, C. Dedonder, C. Jouvet, K. Sakota, and H. Sekiya, Phys. Chem. Chem. Phys. **13**, 6325 (2011).
[36] K. Sakota, Y. Komoto, M. Nakagaki, W. Ishikawa, and H. Sekiya, Chem. Phys. Lett. **435**, 1 (2007).
[37] K. Sakota, N. Inoue, Y. Komoto, and H. Sekiya, J. Phys. Chem. A **111**, 4596 (2007).
[38] K. Sakota, N. Komure, W. Ishikawa, and H. Sekiya, J. Chem. Phys. **130**, 224307 (2009).
[39] H. Sekiya and K. Sakota, J. Photochem. Photobiol. C **9**, 81 (2008).
[40] X. Zhang, Y. Komoto, K. Sakota, N. Masayuki, T. Shinmyozu, S. Nanbu, H. Nakano, and H. Sekiya, Chem. Phys. Lett. **443**, 194 (2007).
[41] M. Mukherjee, S. Karmakar, and T. Chakraborty, J. Phys. Chem. A **115**, 1830 (2011).
[42] A. N. Oldani, J. C. Ferrero, and G. A. Pino, Phys. Chem. Chem. Phys. **11**, 10409 (2009).
[43] R. Ahlrichs, M. Bar, M. Haser, H. Horn, and C. Kolmel, Chem. Phys. Lett. **162**, 165 (1989).
[44] F. Weigend, M. Haser, H. Patzelt, and R. Ahlrichs, Chem. Phys. Lett. **294**, 143 (1998).
[45] O. Christiansen, H. Koch, and P. Jorgensen, Chem. Phys. Lett. **243**, 409 (1995).
[46] D. E. Woon and T. H. Dunning, Jr., J. Chem. Phys. **98**, 1358 (1993).
[47] C. M. Western, PGOPHER, a program for simulating rotational structure, University of Bristol, see http://pgopher.chm.bris.ac.uk./.
[48] Y. Huang, S. Arnold, and M. Sulkes, J. Phys. Chem. **100**, 4734 (1996).

[49]I. Alata, M. Broquier, C. Dedonder-Lardeux, C. Jouvet, M. Kim, W. Yong-Sohn, S-Su Kim, H. Kang, M. Schütz, A. Patzer, and O. Dopfer, J. Chem. Phys. **134**, 074307 (2011).
[50]I. Alata, C. Dedonder, M. Broquier, E. Marceca, and C. Jouvet, J. Am. Chem. Soc. **132**, 17483 (2010).
[51]G. Grégoire, C. Dedonder-Lardeux, C. Jouvet, and S. Martrenchard, J. Phys. Chem. A **104**, 9087 (2000).
[52]See supplementary material at http://dx.doi.org/10.1063/1.4789426 for optimized geometries and relevant bond distances of the 7AI-PhOH complex in the S_0 and S_1 states; and optimized geometries and relevant bond distances of the transition state and final structure of the complex along the CPET (hydrogen transfer) coordinate.
[53]H. Fang and Y. Kim, J. Phys. Chem. A **115**, 13743 (2011).
[54]M. N. R. Ashfold, B. Cronin, A. L. Devine, R. N. Dixon, and M. G. D. Nix, Science **312**, 1637 (2006).
[55]A. L. Sobolewski, W. Domcke, and C. Hattig, Proc. Natl. Acad. Sci. U.S.A. **102**, 17903 (2005).
[56]C. Tanner, C. Manca, and S. Leutwyler, Science **302**, 1736 (2003).